J Paleolimnol (2016) 55:289–302
DOI 10.1007/s10933-016-9880-8

ORIGINAL PAPER

Early–middle Holocene hydroclimate changes in the Asian monsoon margin of northwest China inferred from Huahai terminal lake records

Zhuolun Li · Nai'ang Wang · Hongyi Cheng · Yu Li

Received: 12 April 2015 / Accepted: 1 February 2016 / Published online: 5 February 2016

Abstract In the Asian monsoon margin of northwest China, millennial-scale precipitation and effective moisture changes during the Holocene differ from those observed in the primary monsoon area. Whether these differences were caused by a change in precipitation or other hydroclimate factors remains controversial. We selected Huahai Lake, located in the western portion of the Hexi Corridor, at the northwest margin of the Asian monsoon area, to address this question. Using paleoclimate proxies (mineralogical assemblages and immobile elements) and results from a previous study, we inferred hydroclimate changes in this area during the early and middle Holocene (10.5–5.5 cal ka BP). Heavy precipitation and abundant runoff occurred during the early Holocene (10.5–8.8 cal ka BP). Proxies (carbonate content, total organic carbon and C/N) for precipitation minus evaporation (P − E) in the same section, however, revealed low P − E during the early Holocene and highest P − E in the middle Holocene (8.8–5.5 cal ka BP). Therefore, on a millennial timescale, precipitation amount and effective moisture changes were asynchronous during the early and middle Holocene. The precipitation and effective moisture pattern in the study area during that time span was different from patterns in both the Asian monsoon and westerly wind-influenced areas, suggesting an interplay between the two climate features. High precipitation during the early Holocene corresponded to a strengthened Asian monsoon. Highest P − E in the study area occurred during the middle Holocene and may have been caused by low evaporation, rather than high precipitation.

Keywords Holocene · Asian monsoon · Effective moisture · Precipitation · Northwest China

Z. Li (✉) · N. Wang · H. Cheng · Y. Li
College of Earth and Environmental Sciences, Center for Desert and Climatic Change in Arid Region, Lanzhou University, Lanzhou 730000, China
e-mail: lizhuolunlzl@163.com

Introduction

The Holocene hydroclimate in the Asian monsoon marginal area of northwest China is associated with the Asian monsoon and westerly variability (Li et al. 2012a), and differs from that in both the typical Asian monsoon and westerly areas (Long et al. 2010; Wang et al. 2013b; Li et al. 2015c). In the typical Asian monsoon area, proxy records indicate that precipitation amount and effective moisture content (precipitation minus evaporation) in the early Holocene were higher than during the middle Holocene. A strong summer monsoon and high P − E characterized the early Holocene, whereas a weakened summer monsoon and lower P − E prevailed during the late Holocene (Zhang et al. 2011; Bird et al. 2014). Although the environmental changes in the area

influenced by westerly winds were out of phase with those in monsoonal Asia, the P − E was lower during the early Holocene than in the middle and late Holocene (Chen et al. 2008). However, in the monsoon-westerly transition region of northwest China, a shift from low P − E to high P − E occurred during the early Holocene. Highest P − E conditions occurred during the middle Holocene and lower P − E conditions were dominant during the late Holocene (Zhang et al. 2000; Li et al. 2009, 2015c; Long et al. 2010; Wang et al. 2013b). Differences between these records indicate that the Holocene moisture patterns in the northwest marginal area of the Asian monsoon remain controversial.

Moreover, effective moisture was influenced by several hydroclimate factors, including both precipitation and evaporation. Most of the proxy climate records in previous studies indicated millennial-scale moisture changes in the northwest marginal area of the Asian monsoon (Zhang et al. 2000; Chen et al. 2008; Li et al. 2009; Long et al. 2010; Wang et al. 2013b). Nevertheless, the amount of precipitation at such time scales characterized the strength of the Asian monsoon in the area of influence (Yuan et al. 2004; Wang et al. 2005). It remains uncertain as to whether a low or high P − E environment existed during the early Holocene in this area, influenced by multiple hydroclimatic factors. Furthermore, the linkage between precipitation and variations in the Asian monsoon during the early and middle Holocene in the northwest marginal area of the Asian monsoon requires detailed study.

Huahai Lake is located in the western portion of the Hexi Corridor, northwest China. Current water vapor transport in the Hexi Corridor indicates that Huahai Lake is located in the northwest margin of the Asian monsoon region and that summer precipitation in this area is affected by the westerly winds (Wang et al. 2006, 2013b; Li et al. 2012a). The boundary of the summer monsoon during the Holocene, however, has been in the area between the margin of the north Tibet Plateau and the Tianshan Mountains in Xinjiang (Herzschuh 2006; Chen et al. 2008), indicating that the summer monsoon was the source of moisture in the past (Herzschuh 2006; An et al. 2012). Hence, this is a critical area for study of millennial-scale water vapor transport and Asian monsoon changes at the northwest margin of the monsoon region. Previous research focused on paleoclimate proxies from the Huahai Lake section (HH), dated using 18 ^{14}C samples. The environmental significance of mirabilite deposition in the HH section was described elsewhere (Wang et al. 2003, 2012) and the Holocene effective moisture changes and the lake's evolution were also reconstructed (Wang et al. 2013b). Variations in hydroclimate during the early and middle Holocene, however, remain unclear. This study addresses millennial-scale climate changes in the northwest margin of the Asian monsoon region, using paleoclimate proxies (variability of mineralogical assemblages and immobile elements) to reconstruct changes in precipitation and runoff during the early and middle Holocene.

Study site

Huahai Lake is a playa lake located in the Huahai Basin of the Hexi Corridor, northwest China (Fig. 1a, b), and is the terminal lake of the east tributary of the Shule River (Fig. 1b). The lake covered an area of $\sim$3 km^2 in 1965, but has been dry since 1999, because of water diversion from the middle reaches of the basin for irrigation and other uses, leaving the lakebed exposed on the margins of the Gobi Desert.

The lake basin has an area of 1.44 $\times$ 10^4 km^2, is approximately 40 km from north to south and 70 km from east to west, and lies at 1150–1250 m asl. In terms of geomorphic units, Huahai Lake Basin belongs to the alluvial plain in the middle reach of the Shule River. The landscape around the basin is largely characterized by slopes and extensive plains. The alluvial and lacustrine plains are distributed along the eastern branch of the Shule River. Geologically, the Huahai Lake Basin belongs to a Cenozoic foreland basin system on the northeastern margin of the Tibet Plateau, which extends northeastward (Tapponnier et al. 2001). The lithology in and around the basin is characterized by clastic rocks, with limestone and small quantities of metamorphic and igneous rocks. There are mountains of low to medium height along the southern edge of the basin, such as the Kuantan and Heishan Mountains, with elevations of 2243–2799 m. The northern edge of the basin is part of the Beishan Mountains, which are denuded and lie at elevations between 1400 and 1900 m. The basin is free from direct influence of the Asian summer monsoon, and the present-day climate is extremely dry and continental (Wang et al. 2006; Li et al. 2012a). Meteorological data indicate an annual average temperature of

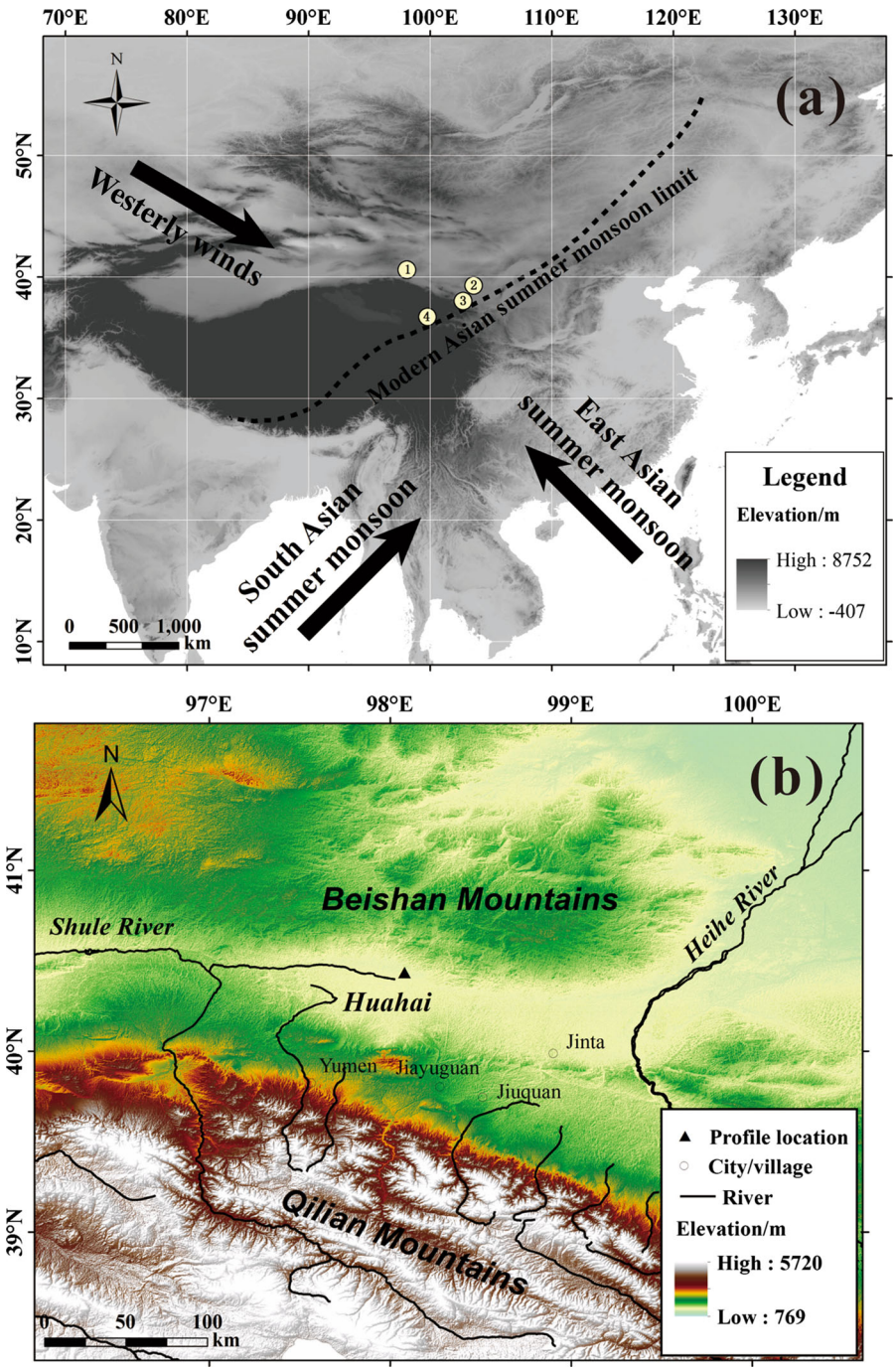

Fig. 1 Location of the study area. **a** Current climate systems of the study area and East Asia (*1* is Huahai Lake, *2* is Zhuye Lake, *3* is Hongshui River, and *4* is Qinghai Lake). **b** Study area topography and HH section location

8 °C and average temperatures for January/July of −9/22 °C (Fig. 2). The average annual precipitation in Huahai Basin is approximately 65 mm, 52 % of which is concentrated in summer (from June to August), whereas an average of 5 mm occurs in winter (Fig. 2). Mean annual evaporation is approximately 3000 mm (Chen 2010).

The Shule River (40°11′–40°34′N, 96°30′–97°40′E) and its east tributary, which flows into Huahai Lake, originates in the Qilian Mountains at an

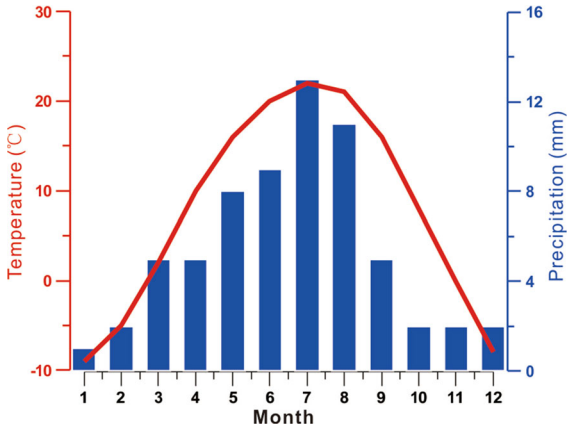

Fig. 2 Modern monthly temperature and precipitation distributions at Huahai Lake (from Yumen Station meteorological data)

elevation of ~4800 m, and is the inland river basin in the arid region of northwest China (Wang et al. 2015). The upper reaches, with annual precipitation of 300–400 mm and evaporation of 900–1300 mm, are the primary areas for runoff (Li et al. 2015a). The annual runoff of the river from the mountain areas is 16.7×10^8 m^3, including ice/snow-melt water, precipitation, and groundwater. Among these, precipitation is the main supply (Lan et al. 2012; Li et al. 2015a), causing fluctuations in runoff along the upper reaches of the Shule River Basin that correspond to precipitation variation (Lan et al. 2012). Runoff, air temperature, and precipitation data from 1960 to 2010 reveal that streamflow is sensitive to climate change (Wang et al. 2013a).

Materials and methods

Sample collection and lithologic description

The 17.25-m-thick HH section (40°26′05″N, 98°04′47″E) is located in the lowest part of the Huahai Lake Basin (Fig. 1b). Sediments of the HH can be lithologically divided into 12 layers (Wang et al. 2012, 2013b). The sequence chronology was developed using 18 ^{14}C dates on bulk organic matter and plant remains (Wang et al. 2013b). Plant parts and seeds in plant residues were from *Ruppia maritima* (Potamogetonaceae), a submersed taxon. The "reservoir effect" in Huahai Lake is ~2500 years, according to the ^{14}C age difference between terrestrial plant residues (twigs) and bulk organic matter from the same layer at 9.25 m depth (Wang et al. 2012). This age offset is considered to have been constant as far as its influence on reconstruction of millennial-scale Holocene environmental changes in Huahai Lake (Wang et al. 2013b). Although this assumption may contribute some error to the section chronology, it is probably not critical for reconstruction of millennial-scale Holocene environmental change (Wang et al. 2013b). All ^{14}C ages, except those from the top alluvial layers, were therefore corrected for the "reservoir effect" (2500 years) prior to calibrating them to calendar year ages (Fig. 3).

The Holocene sedimentary facies in the HH section (Fig. 3) were described as follows (Wang et al. 2013b): 0–0.73 m corresponds to alluvial deposition with light red or brown-yellow clayey silt, partially covered by modern wind-blown sand; 0.73–3.73 m reflects lacustrine deposition with gray and grayish-white bedded clayey silt; 3.73–4.53 m represents alluvial deposition with light brown or brown clayey silt; 4.53–5.25 represents aeolian deposition with gray-yellow aeolian silt-fine sand; 5.25–6.30 m represents alluvial deposition with deep tan and purple-brown granular clayey silt. Therefore, Holocene alluvial and aeolian deposition events (6.30–3.73 m) occurred before 10.5 cal ka BP with a high deposition rate (Fig. 3a–c). Lacustrine deposition (3.73–0.73 m) prevailed from 10.5 to 5.5 cal ka BP (Fig. 3d), but thereafter there was a lacustrine depositional hiatus (Fig. 3e). Moreover, the lacustrine sediment was deposited at the rate of 0.4 m/ka in the 3.73–3.08 m depth interval (10.5–8.8 cal ka BP), and 0.5 m/ka in the 3.08–0.73 m depth interval (8.8–5.5 cal ka BP). A total of 153 samples were collected from 8.42 to 0.40 m depth, at 5-cm intervals in the lacustrine sediment layers and at 10-cm intervals in the sand layer.

Laboratory methods

Qualitative and semi-quantitative analyses of mineralogical assemblages were conducted using X-ray diffraction (XRD), following the procedures described in Moore and Reynolds (1997) and Last (2001). Mineral diffraction patterns were collected with an X-Pert Pro X-ray diffractometer (X'Pert Pro MPD, Phillips). Then, the identified species and relative

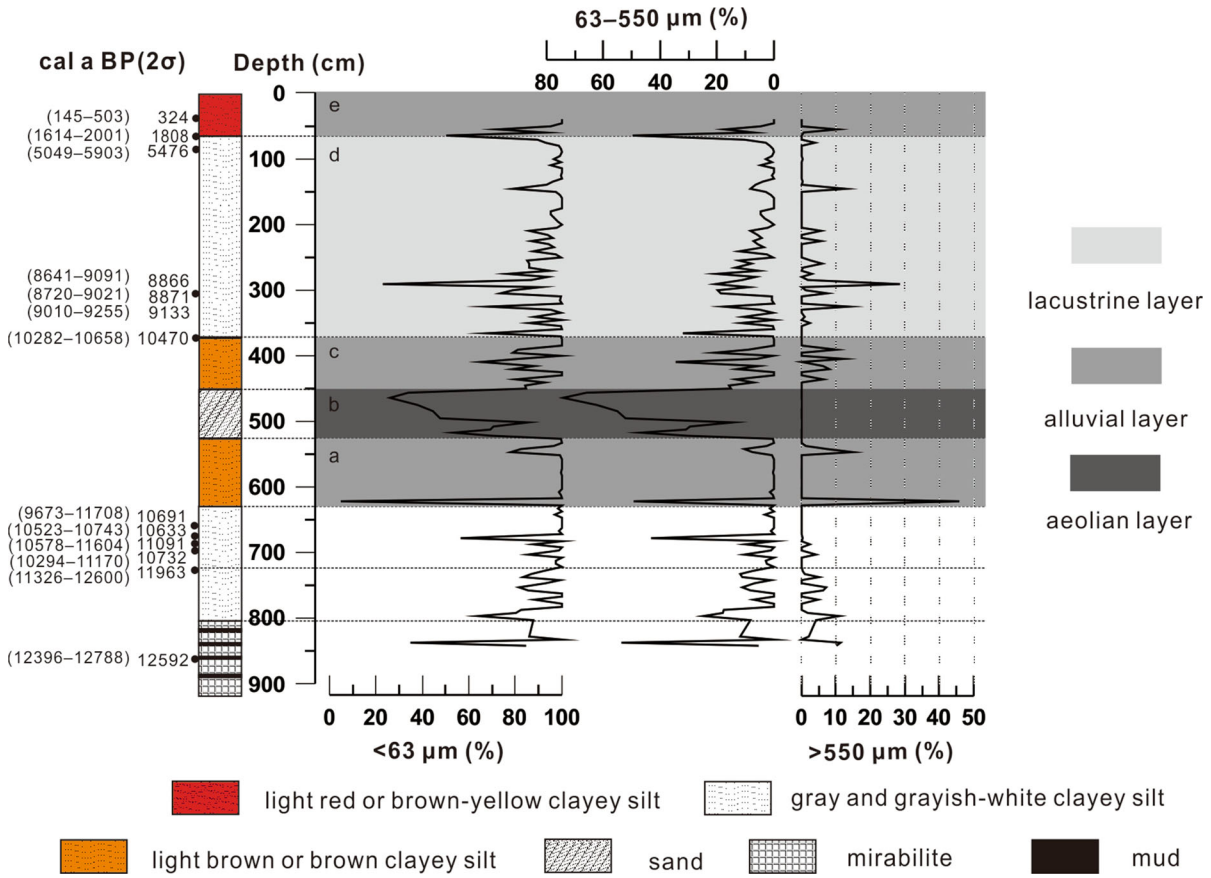

Fig. 3 Grain-size distribution in the HH section from Wang et al. (2013b). Phase *a* (6.30–5.25 m), phase *c* (4.53–3.73 m) and phase *e* (0.73–0 m) were alluvial depositions; phase *b* (5.25–4.53 m) was an aeolian deposition and phase *d* (3.73–0.73 m) was a lacustrine deposition

component contents were assessed using X'Pert High Score Plus software. Weight percentages of the minerals were calculated as

$$X_i = \left(\frac{K_{i,n}}{I_{i,n}} \sum_{j=1}^{m} \frac{I_{j,n}}{K_{j,n}} \right)^{-1} \quad (1)$$

where X_i is the weight percentage of mineral i, $K_{i,n}$ and $K_{j,n}$ are the intensity ratios of minerals i and j in the diffracted ray n, $I_{i,n}$ and $I_{j,n}$ are the integrated intensity of minerals i and j in the diffracted ray n, and m is the number of all minerals. Trace minerals were excluded because semi-quantitative XRD estimates involve a 5 % uncertainty. The weight percentage of the total exogenous detrital mineral corresponded to the sum of quartz, feldspar, mica, and clinochlore percentages. The weight percentage of the total saline minerals was obtained through the sum of carbonate, sulfate, and halide salt mineral contributions.

Geochemical elemental analyses, focusing on Al, Si, Y, Ti, Fe and Rb, were conducted by means of X-ray fluorescence spectrometry (XRF), using a Magix PW2403 spectrometer. Prior to analysis, the samples were dried, ground, and sifted through a 200-mesh screen. Then, 4-g fractions of powdered samples were placed in a mold with boric acid at the edge and bottom, and pressed into 32-mm-diameter round discs under 30-ton pressure at 105 °C. The XRF measurements used a super-long, sharp-pointed ceramic X-ray light tube (4-kW power) and a pipe flow of 160 mA. The estimated error was <5 %.

Results

X-ray diffraction results show that the main minerals in the HH section characterize both detrital and saline species. The detrital minerals include quartz, mica,

feldspar, and chlorite, whereas the saline types include calcite, dolomite, and gypsum. Average detrital mineral content in Holocene lake sediments (3.73–0.73 m) was 71 %, but varied from 34 to 85 % (Fig. 4). Total detrital mineral content increased in the early Holocene (3.73–3.08 m, 10.5–8.8 cal ka BP), with an average of 79.4 %, followed by a sudden decrease to the lowest value after 8.8 cal ka BP (Fig. 4). Although total detrital mineral content increased in the middle Holocene (3.08–0.73 m, 8.8–5.5 cal ka BP), with an average of 67.4 %, it remained lower than early Holocene values.

Concentrations of Al, Y, Ti, Fe and Rb increased in the early Holocene lacustrine deposits (3.73–3.08 m), whereas Si content decreased during the same period (Fig. 5). Concentrations of all immobile elements declined abruptly to the lowest value after 8.87 cal ka BP. Thereafter, concentrations increased during the middle Holocene (3.08–0.73 m, 8.8–5.5 cal ka BP), but remained lower than values in early Holocene lacustrine deposits (3.73–3.08 m).

Discussion

Proxy interpretation

Detrital mineral input to lakes of arid regions in China is influenced by both runoff and wind transport. An increase in precipitation generally enhances soil erosion and transport capacity of streams and rivers across the drainage area, leading to runoff transport of detrital minerals into the lake, thereby increasing their relative abundance in the sediment (Long et al. 2010; Dietze et al. 2013; Wang et al. 2013b; Li et al. 2014). Moreover, strengthening wind force can also increase detrital input (Yao et al. 2011; Li et al. 2014). Wang et al. (2013b) pointed out the three main components of grain-size distribution in the HH section sediments: <63, 63–550 and >550 μm. Hu et al. (2002) suggested there was an aeolian component, characterized by a rounded, well-sorted texture and modal grain size of about 100–300 μm, with a range of 63–550 μm. Figure 3 reveals a 0–20 % aeolian input (63–550 μm) in the lake sediments (3.73–0.73 m), with <10 % predominance in most layers, indicating a minor contribution of this source to the overall detrital mineral content. Consequently, variations in detrital mineral content at Huahai Lake mainly reflect shifts in delivery of river-transported sediments. Assuming that source did not vary, high detrital mineral content indicates increased runoff. During the Holocene, Huahai was the terminal lake of the Shule River east tributary, and the catchment remained nearly unchanged. Therefore, we interpret the content of detrital minerals in the HH section sediments as a proxy for runoff variation. High detrital mineral content reflects increased runoff during the Holocene, whereas low mineral content is indicative of decreased runoff.

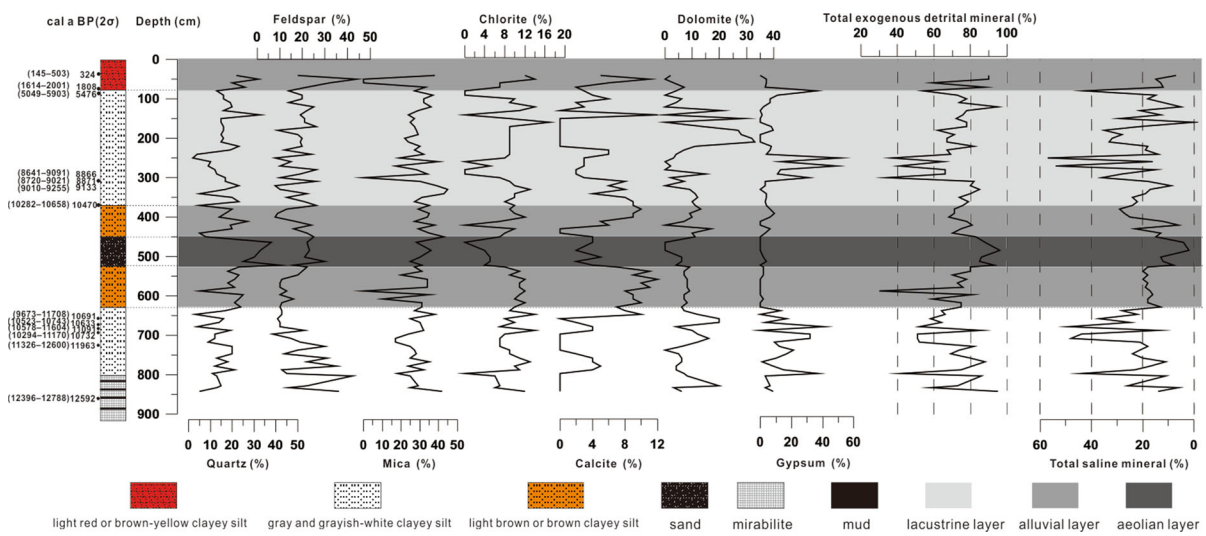

Fig. 4 Mineralogical assemblage variability in the HH section

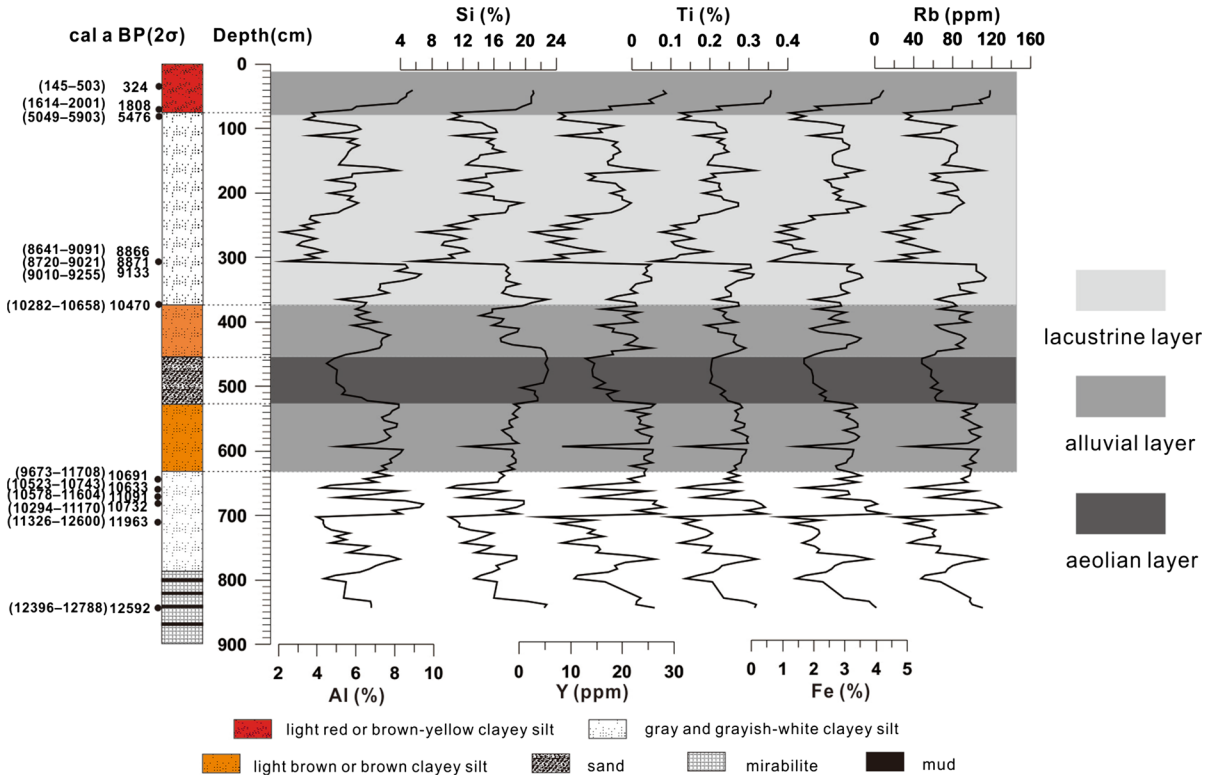

Fig. 5 Variability of Al, Si, Y, Ti, Fe, and Rb elements in the HH section

Immobile elements, including Al, Si, Y, Ti, Fe, and Rb, are usually substituted in the structural sites of rock-forming minerals. During weathering, soluble and climate-sensitive species, such as Ca^{2+}, Na^{+} and K^{+} (Chang et al. 2013; Liu et al. 2014), are leached more easily than immobile elements (Nesbitt and Young 1989). The stable elements are quite abundant in clay and mainly exist in the residual phases (Koinig et al. 2003; Jin et al. 2006). The amount of stable elements leached from catchments is small and does not change perceptibly as the climate changes in the arid region of China (Chang et al. 2013; Zeng et al. 2013). Input of immobile elements into the lakes is influenced by erosion (Zeng et al. 2013; Zhang et al. 2015) and the erosion rates in the study area during the Holocene were controlled by precipitation at the millennial scale (Li et al. 2012b). Therefore, we interpreted the HH sediment Al, Si, Y, Ti, Fe, and Rb chemical content as a proxy for precipitation amount. A high concentration of immobile elements reflects high precipitation during the Holocene, and vice versa.

Multi-hydroclimate changes in the Huahai Lake during the early and mid-Holocene

Results indicate there were two stages of hydroclimate variation in Huahai Lake during the early and middle Holocene. Stage 1 (10.5–8.8 cal ka BP) corresponds to a period of high precipitation and runoff, as reflected by both high detrital mineral content (Fig. 4) and immobile element concentrations (Fig. 5). Stage 2 (8.8–5.5 cal ka BP) was a period of low precipitation and limited runoff, supported by both decreased detrital mineral content and immobile element concentrations.

In previous investigations, millennial-scale effective moisture changes in Huahai Lake during the Holocene were reconstructed using multiple proxies, such as carbonate content and total organic carbon (TOC) (Wang et al. 2013b). Carbonate content in Huahai Lake reflects lake water salinity, controlled by effective moisture (Wang et al. 2013b). Moreover, higher values of TOC from autochthonous sources indicate increased lacustrine biomass production, also

governed by effective moisture in arid regions (Pedersen and Calvert 1990; An et al. 1993; Long et al. 2010; Wang et al. 2013b). Although carbonate content and TOC in Huahai Lake were used as proxies for effective moisture (Wang et al. 2013b), this climate variable is influenced by both precipitation and evaporation (Wang et al. 2013b), and is probably best interpreted as reflecting the difference between precipitation and evaporation (P − E). Carbonate content and TOC in the Huahai Lake sediment are not direct indicators of precipitation variations, but rather, changes in P − E.

Comparison of results (Fig. 6) indicates that the lowest P − E occurred in the early Holocene (10.5–8.8 cal ka BP) and highest P − E in the middle Holocene (8.8–5.5 cal ka BP). The present study, however, reveals higher total detrital mineral content and immobile element concentrations in the early Holocene lacustrine deposits (3.73–3.08 m) than in middle Holocene sediments (3.08–0.73 m), indicating heavy precipitation and large amounts of runoff during the early Holocene (10.5–8.8 cal ka BP), and the opposite case during the middle Holocene (Fig. 6). Thus, different climate proxies from the same section indicate asynchronous variations in precipitation and P − E occurred during the early and middle Holocene, on a millennial timescale.

Comparison with previous studies

To clarify whether the precipitation and P − E records obtained at Huahai Lake reflect local or regional conditions, we compared our results with other proxy records for the NW Asian monsoon margin, the monsoon area of the southern Tibet Plateau and the area influenced by the westerly winds (Fig. 7).

Table 1 lists reconstructions of Holocene hydroclimate changes in the NW Asian monsoon margin. In Zhuye Lake, located in the eastern portion of the Hexi Corridor of the NW Asian monsoon margin, proxy records from lake sediments (grain size, pollen, total organic carbon content and C/N ratios) reflect changes in effective moisture (P − E), indicating increased P − E during early Holocene and highest P − E in the

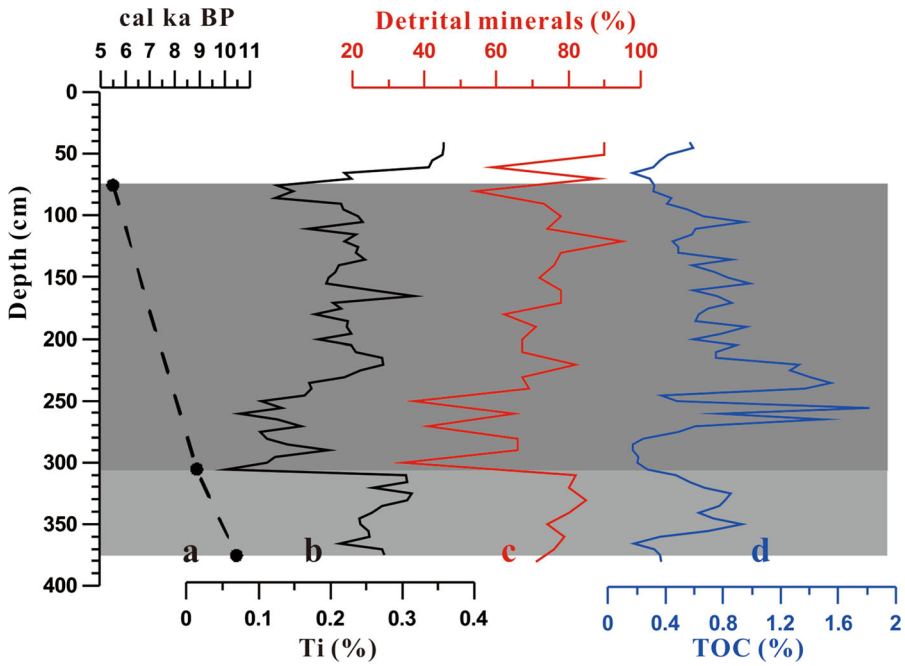

Fig. 6 Hydroclimate changes in Huahai Lake on millennial timescales during the early and middle Holocene. *a* The age-depth plot in the HH section (Wang et al. 2013b), *b black solid line* indicates precipitation changes [content of Ti (%) in the HH section], *c red line* indicates variations in runoff amount [content of detrital minerals (%) in the HH section], and *d blue line* indicates effective moisture (P − E) changes [TOC content in the HH section (Wang et al. 2013b)]. *Lighter shading* and *darker shading* refer to early Holocene (10.5–8.8 cal ka BP) and middle Holocene (8.8–5.5 cal ka BP), respectively. (Color figure online)

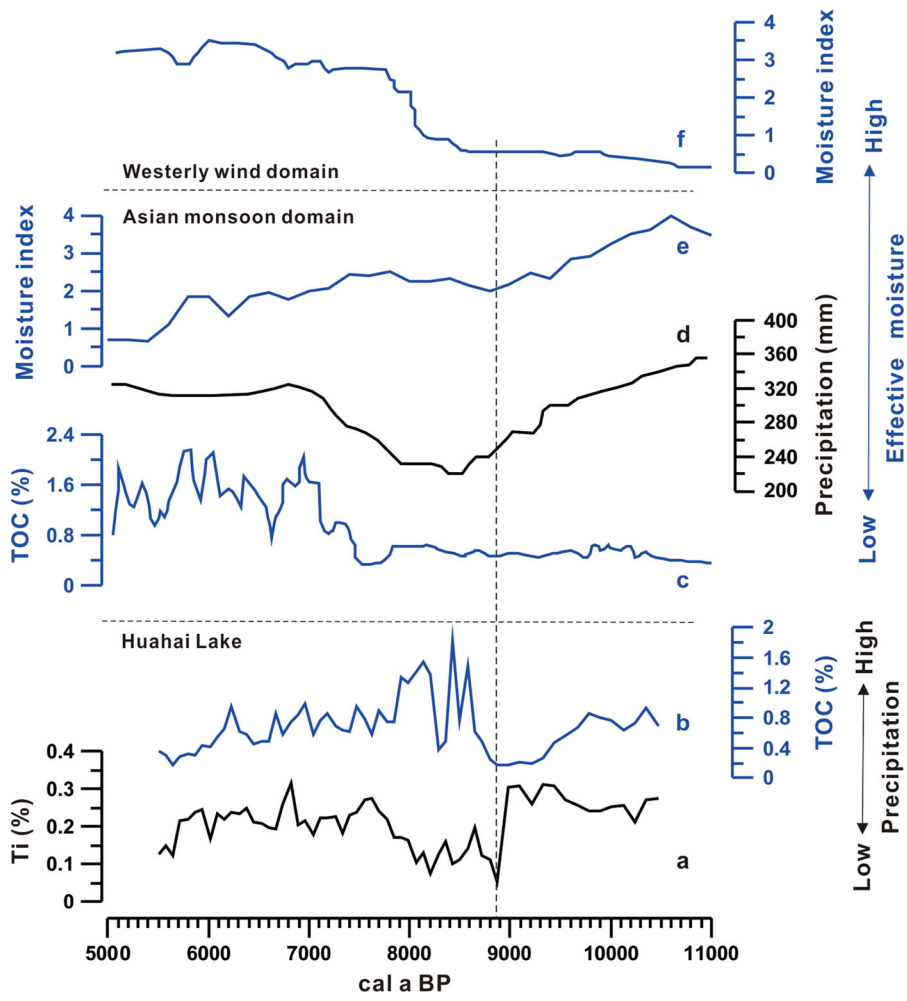

Fig. 7 Comparison of our study with other Holocene paleoclimate records from the Asian monsoon domain and the westerly wind domain. *a* Ti (%) in the HH section, *b* TOC (%) in the HH section (Wang et al. 2013b), *c* TOC (%) in the section from Zhuye Lake, located in the eastern portion of the Hexi Corridor (Li et al. 2009), *d* quantitative reconstruction of precipitation changes at Donggi Cona Lake (Wang et al. 2014), *e* changes in effective moisture (P − E) index on the Tibet Plateau (Ran and Feng 2013) and *f* average humidity index for 11 lakes in Central Asia (Chen et al. 2008). *Black line* indicates precipitation changes; *blue line* indicates effective moisture (P − E) changes. (Color figure online)

middle Holocene (Li et al. 2009; Long et al. 2010). Lake-level variations in this area during the Holocene also reflect changes in effective moisture (P − E) (Li and Morrill 2010). Geomorphic shoreline investigations suggested that high lake levels existed in the middle Holocene, with the highest P − E stage of the Holocene occurring in this period (Zhang et al. 2004; Wang et al. 2011; Long et al. 2012). In Hongshui River (Table 1), also located in the eastern portion of the Hexi Corridor of the NW Asian monsoon margin, stratigraphic and chronologic studies revealed that the highest P − E occurred between 7.5 and 5.1 cal ka BP (Zhang et al. 2000). Moreover, in the Tengger Desert, effective moisture affects the formation of calcareous root tubes, and their presence indicates relatively humid conditions (Li et al. 2015b). Using ^{14}C dates on Holocene calcareous root tube samples, Li et al. (2015c) suggested that the highest effective moisture (P − E) in the Tengger Desert occurred in the 8–5 cal ka BP period. In Qinghai Lake, influenced by the Asian summer monsoon during the late Quaternary (An et al. 2012), lake levels were relatively low during 11–8 ka, rose substantially after 8 ka, and reached a Holocene high stand at 5 ka (Liu et al. 2015). Furthermore, quantitative reconstruction of precipitation changes on Donggi Cona Lake, in the northeastern part of the Tibet Plateau, revealed that precipitation increased to a 400 mm/year peak during the early Holocene (Fig. 7), whereas the period of second highest precipitation occurred in the middle Holocene (340 mm/year) (Wang et al. 2014). These results agree with the present study, demonstrating a highest precipitation stage during the early Holocene. Therefore, results in Table 1 shows that the

Table 1 Millennial-scale Holocene hydroclimate changes in the NW Asian monsoon margin

Location	Section	Records	Proxy interpretations	Early Holocene	Mid-Holocene	References
39°03′N, 103°40′E	Zhuye Lake	Grain size, carbonate, TOC, C/N and $\delta^{13}C$ of organic matter from Lake sediments	Effective moisture (P − E)	P − E increased (9.5–7 cal ka BP)	Highest stage of P – E (7.0–4.8 cal ka BP)	Long et al. (2010)
39°03′N, 103°40′E	Zhuye Lake	Pollen from Lake sediments	Effective moisture (P − E)	P − E increased (11.0–7.4 cal ka BP)	Highest stage of P − E (7.4–4.7 cal ka BP)	Li et al. (2009)
39°08′N, 104°08′E	Zhuye Lake	Lake shorelines	Effective moisture (P − E)	–	Highest stage of P – E (7.0–4.8 cal ka BP)	Zhang et al. (2004), Wang et al. (2011) and Long et al. (2012)
38°10′N, 102°45′E	Hongshui River	TOC, Total inorganic carbon (TIC), element composition and pollen from the sediments	Effective moisture (P − E)	P − E increased (8.45–7.5 cal ka BP)	Highest stage of P – E (7.5–5.07 cal ka BP)	Zhang et al. (2000)
37°55′N–39°10′N 103°31′E–105°23′E	The Tengger Desert	Calcareous root tubes	Effective moisture (P − E)	Low P – E (∼8 cal ka BP)	Highest stage of P – E (8–5 cal ka BP)	Li et al. (2015c)
40°26′N, 98°04′E	Huahai Lake	Carbonate content and TOC	Effective moisture (P − E)	P − E increased (10.4–8.8 cal ka BP)	Highest stage of P – E (8.8–5.5 cal ka BP)	Wang et al. (2013b); This study
36°50′N, 99°42′E	Qinghai Lake	Lake shorelines	Effective moisture (P − E)	Low P − E (11–8 cal ka BP)	Highest stage of P – E (8–5 cal ka BP)	Liu et al. (2015)
35.22°–35.83°N, 98.33°–98.75°E;	Donggi Cona Lake	Pollen	Precipitation	Highest precipitation (11–9 cal ka BP)	Second highest precipitation (7–4.5 cal ka BP)	Wang et al. (2014)
40°26′N, 98°04′E	Huahai Lake	Geochemical element	Precipitation	Highest precipitation (10.4–8.8 cal ka BP)	Precipitation decreased (8.8–5.5 cal ka BP)	This study

millennial-scale changes in effective moisture (P − E) and precipitation in the NW Asian monsoon margin were asynchronous. Highest precipitation occurred in the early Holocene, whereas highest P − E occurred in the middle Holocene.

In the monsoon area of the southern Tibet Plateau, Hudson and Quade (2013) suggested that the greatest "paleo" rainfall occurred during the early Holocene, then progressively declined throughout the middle and late Holocene. Other investigations (Opitz et al. 2012; Dietze et al. 2013; Herzschuh et al. 2014; Hudson et al. 2015; Huth et al. 2015) suggested a similar trend. Moreover, Morrill et al. (2003) compiled previously published paleoclimate records to determine the timing and spatial pattern of the abrupt, century-scale changes in Asian monsoon precipitation since the last deglaciation. At the start of the Holocene (∼11.5 cal ka BP), the Asian monsoon precipitation increased dramatically. Feng et al. (2006) suggested that a warmer environment with high effective

moisture (P − E) occurred during the early and middle Holocene (~10.5–10 to ~5–4 cal ka BP) on the Tibet Plateau. Recently, Ran and Feng (2013) reviewed effective moisture (P − E) changes during the Holocene on the Tibet Plateau, which extended to ~11.5 cal ka BP, with optimum moisture lasting from approximately ~11.5 to ~7.5 cal ka BP (Fig. 7). These reviews (Morrill et al. 2003; Feng et al. 2006; Ran and Feng 2013) and previous research suggested that changes in precipitation and effective moisture (P − E) underwent synchronous variations during the early and middle Holocene.

In the area influenced by westerly winds, reconstructed Holocene effective moisture reveals lower P − E during the early Holocene than in the middle and late Holocene (Chen et al. 2008) (Fig. 7). Changes in P − E were out of phase with those in the monsoon area (Chen et al. 2008; Zhang et al. 2011). At Wulungu Lake in China, lowest P − E occurred between 9.6 and 6.8 cal ka BP (Liu et al. 2008), and at Bosten Lake in China, aeolian sand was deposited before 8.4 cal ka BP. This depositional typology indicates dried lake conditions and predominant low effective moisture (P − E) during this period (Wünnemann et al. 2006; Huang et al. 2009). Chronostratigraphic results of an aeolian sedimentary sequence from Bayanbulak Basin (Xinjiang, NW China) also pointed towards a low P − E climate condition, characterized by sand dune accumulation at ~9–8 ka (Long et al. 2014). Moreover, model simulation results validated this low P − E climate event during the early Holocene (11–8 ka) in mid-latitude central Asia (Jin et al. 2012). Therefore, P − E changes in the westerly wind-influenced area suggest that low P − E conditions prevailed in the early Holocene, and high P − E conditions were dominant during the middle Holocene, which differs from the situation at Huahai Lake.

Thus, millennial-scale precipitation variations at Huahai Lake and the southern Tibet Plateau Monsoon areas were synchronous during the early and middle Holocene. However, effective moisture (P − E) variations were asynchronous: in the southern Tibet Plateau Monsoon areas, the most humid conditions occurred during the early Holocene, whereas they occurred in the middle Holocene at Huahai Lake (Wang et al. 2013b), in the NW Asian monsoon margin, including Zhuye Lake in the Hexi Corridor (Long et al. 2010), and at Qinghai Lake on the northeast Tibet Plateau (Liu et al. 2015). Moreover, the millennial-scale precipitation and effective moisture (P − E) variations in the NW Asian monsoon margin were out of phase with those in the areas affected by westerly winds.

Probable forcing mechanisms of Holocene hydroclimate change

This study demonstrates that Holocene hydroclimate changes on millennial timescales involved high precipitation and large amounts of runoff during the early Holocene, whereas the highest P − E occurred during the middle Holocene. The pattern of asynchronous changes in precipitation and P − E between the early and middle Holocene is different from that in a typical Asian monsoon area, and in the area influenced by westerly winds (Fig. 7). The discrepancy is most likely related to the asynchronous changes in evaporation and monsoon precipitation rates.

According to current monsoon climate research, modern monsoon precipitation does not reach the northeastern Tibet Plateau (Aggarwal et al. 2004; Drumond et al. 2011). The modern northwestern edge of the Asian summer monsoon water vapor transport is located in the eastern Qilian Mountains of northwest China (Wang et al. 2006; Li et al. 2012a). However, the northern monsoon boundary can shift, in response to millennial-scale climate changes (Li et al. 2013), lying in the area between the margin of the north Tibet Plateau and the Tianshan Mountains in Xinjiang, during the Holocene (Herzschuh 2006; Chen et al. 2008). The Asian summer monsoon strengthened in the Late Glacial and maintained its intensity until the early to mid-Holocene (Wang et al. 2010), affected by the combined effects of variations in both low-latitude solar radiation and ITCZ position. During the early Holocene, strong summer monsoons led to a relatively large increase in precipitation in monsoon areas, including the Hexi Corridor and the Tibet Plateau, leading to associated, large runoff amounts that affected Huahai Lake. Therefore, the reconstructed high precipitation during the early Holocene is consistent with the same effect in the monsoon area of the Tibet Plateau (Fig. 7), corresponding to a strengthened Asian monsoon during the early Holocene.

During the middle Holocene, changes in precipitation and P − E at Huahai Lake were different from those on the Tibet Plateau, at the millennial timescale. The precipitation decreased in the middle Holocene,

compared to the early Holocene and was consistent with fluctuations in the Indian monsoon, indicating that water vapor transport may have been monsoon-sensitive, whereas results of P − E reconstruction indicated that the highest P − E environment occurred during the middle Holocene (Wang et al. 2013b). This difference may arise from two factors. First, greatly enhanced evaporation (E), even relative to higher monsoon precipitation (P) in arid lands during the early Holocene, may have reduced the effective humidity (Long et al. 2010). The highest summer air temperatures occurred in the early Holocene, as revealed by Long et al. (2010) and Marcott et al. (2013), possibly leading to enhanced evaporation. On the other hand, low evaporation in Central and East Asia could have caused P − E to increase during the middle Holocene (Li and Morrill 2010). Thus, asynchronous changes in precipitation and effective moisture (P − E) on a millennial timescale during the early and middle Holocene at Huahai Lake could have been caused by asynchronous changes in evaporation and monsoon precipitation rates.

Conclusions

The combination of geochemical and mineralogical climate proxies, coupled with previous results, enabled reconstruction of millennial-scale hydroclimate variations at Huahai Lake during the early and middle Holocene (10.5–5.5 cal ka BP). From 10.5 to 8.8 cal ka BP, precipitation, runoff amount and effective moisture (P − E) increased. From 8.8 to 5.5 cal ka BP, precipitation and runoff amount decreased, while P − E increased, resulting in the highest P − E environment of this period.

Asynchronous changes in precipitation and P − E at Huahai Lake on a millennial timescale, during the early and middle Holocene, suggest a precipitation increase during the early Holocene, whereas P − E was highest in the middle Holocene. This precipitation and P − E pattern in the study area during the Holocene is different from that in the Asian monsoon area, or the westerly wind-influenced area, suggesting an interplay between the monsoon and westerly winds.

Asynchronous changes at Huahai Lake concerning precipitation and P − E values on a millennial timescale during the early and middle Holocene, could have been caused by asynchronous changes in evaporation and monsoon precipitation rates. Highest precipitation during the early Holocene corresponded to a strengthened Asian monsoon. Highest P − E in the study area, however, occurred during the middle Holocene, probably caused by lower evaporation rather than higher precipitation.

Acknowledgments Special thanks to Miss Youhong Gao for help drawing Fig. 1. We also thank the editors and the anonymous reviewers for their constructive comments, which led to significant improvement of this manuscript. This study was supported by the National Natural Science Foundation of China (Nos. 41530745, 41301217, and 41371114) and the Fundamental Research Funds for the Central Universities (lzujbky-2015-148).

References

Aggarwal PK, Fröhlich K, Kulkarni KM, Gourcy LL (2004) Stable isotope evidence for moisture sources in the Asian summer monsoon under present and past climate regimes. Geophys Res Lett 31:L08203

An Z, Porter SC, Zhou W, Lu Y, Donahue DJ, Head M, Wu X, Ren J, Zheng H (1993) Episode of strengthened summer monsoon climate of Younger Dryas age on the Loess Plateau of central China. Quat Res 39:45–54

An Z, Colman SM, Zhou W, Li X, Brown ET, Jull AJT, Cai Y, Huang Y, Lu X, Chang H (2012) Interplay between the Westerlies and Asian monsoon recorded in Lake Qinghai sediments since 32 ka. Sci Rep 2:619

Bird BW, Polisar PJ, Lei Y, Thompson LG, Yao T, Finney BP, Bain DJ, Pompeani DP, Steinman BA (2014) A Tibetan lake sediment record of Holocene Indian summer monsoon variability. Earth Planet Sci Lett 399:92–102

Chang H, An Z, Wu F, Jin Z, Liu W, Song Y (2013) A Rb/Sr record of the weathering response to environmental changes in westerly winds across the Tarim Basin in the late Miocene to the early Pleistocene. Palaeogeogr Palaeoclimatol Palaeoecol 386:364–373

Chen X (2010) Physical geography of arid land in China. Science Press, Beijing, pp 286–287 **(in Chinese)**

Chen F, Yu Z, Yang M, Ito E, Wang S, Madsen DB, Huang X, Zhao Y, Sato T, John B, Birks H, Boomer I, Chen J, An C, Wünnemann B (2008) Holocene moisture evolution in arid central Asia and its out-of-phase relationship with Asian monsoon history. Quat Sci Rev 27:351–364

Dietze E, Wünnemann B, Hartmann K, Diekmann B, Jin H, Stauch G, Yang S, Lehmkuhl F (2013) Early to mid-Holocene lake high-stand sediments at Lake Donggi Cona, northeastern Tibetan Plateau, China. Quat Res 79:325–336

Drumond A, Nieto R, Gimeno L (2011) Sources of moisture for China and their variations during drier and -wetter conditions in 2000–2004: a Lagrangian approach. Clim Res 50:215–225

Feng ZD, An C, Wang H (2006) Holocene climatic and environmental changes in the arid and semi-arid areas of China: a review. Holocene 16:119–130

Herzschuh U (2006) Palaeo-moisture evolution in monsoonal Central Asia during the last 50,000 years. Quat Sci Rev 25:163–178

Herzschuh U, Borkowski J, Schewe J, Mischke S, Tian F (2014) Moisture-advection feedback supports strong early-to-mid Holocene monsoon climate on the eastern Tibetan Plateau as inferred from a pollen-based reconstruction. Palaeogeogr Palaeoclimatol Palaeoecol 402:44–54

Hu G, Wang N, Gao S, Li Q, Zhao Q, Guo J (2002) Discovery of Holocene aeolian sand in Huahai Lake and its environmental significance. J Desert Res 22(2):159–165 **(in Chinese with English abstract)**

Huang X, Chen F, Fan Y, Yang M (2009) Dry late-glacial and early Holocene climate in arid central Asia indicated by lithological and palynological evidence from Bosten Lake, China. Quat Int 194:19–27

Hudson AM, Quade J (2013) Long-term east-west asymmetry in monsoon rainfall on the Tibetan Plateau. Geology 41:351–354

Hudson AM, Quade J, Huth TE, Lei G, Cheng H, Edwards LR, Olsen JW, Zhang H (2015) Lake level reconstruction for 12.8–2.3 ka of the Ngangla Ring Tso closed-basin lake system, southwest Tibetan Plateau. Quat Res 83:66–79

Huth T, Hudson AM, Quade J, Guoliang L, Hucai Z (2015) Constraints on paleoclimate from 11.5 to 5.0 ka from shoreline dating and hydrologic budget modeling of Baqan Tso, southwestern Tibetan Plateau. Quat Res 83:80–93

Jin Z, Cao J, Wu J, Wang S (2006) A Rb/Sr record of catchment weathering response to Holocene climate change in Inner Mongolia. Earth Surf Proc Landf 31:285–291

Jin L, Chen F, Morrill C, Otto-Bliesner BL, Rosenbloom N (2012) Causes of early Holocene desertification in arid central Asia. Clim Dyn 38:1577–1591

Koinig KA, Shotyk W, Lotter AF, Ohlendorf C, Sturm M (2003) 9000 years of geochemical evolution of lithogenic major and trace elements in the sediment of an alpine lake—the role of climate, vegetation, and land-use history. J Paleolimnol 30:307–320

Lan Y, Hu X, Xiao S, Wen J, Wang G, Zou S, La C, Song J (2012) Study on climate change in mountainous region of Shulehe River Basin in past 50 years and its effect to mountainous runoff. Plateau Meteorol 31:1636–1644 **(in Chinese with English abstract)**

Last WM (2001) Mineralogy analysis of lake sediments. In: Last WM, Smol JP (eds) Tracking environmental change using lake sediments. Kluwer, Dordrecht, The Netherlands, pp 143–187

Li Y, Morrill C (2010) Multiple factors causing Holocene lake-level change in monsoonal and arid central Asia as identified by model experiments. Clim Dyn 35:1119–1132

Li Y, Wang N, Cheng H, Long H, Zhao Q (2009) Holocene environmental change in the marginal area of the Asian monsoon: a record from Zhuye Lake, NW China. Boreas 38:349–361

Li Y, Wang N, Chen H, Li Z, Zhou X, Zhang C (2012a) Tracking millennial-scale climate change by analysis of the modern summer precipitation in the marginal regions of the Asian monsoon. J Asian Earth Sci 58:78–87

Li Y, Wang N, Morrill C, Anderson DM, Li Z, Zhang C, Zhou X (2012b) Millennial-scale erosion rates in three inland drainage basins and their controlling factors since the Last Deglaciation, arid China. Palaeogeogr Palaeoclimatol Palaeoecol 365–366:263–275

Li Y, Wang N, Li Z, Zhou X, Zhang C (2013) Climatic and environmental change in Yanchi Lake, Northwest China since the Late Glacial: a comprehensive analysis of lake sediments. J Geogr Sci 23:932–946

Li Z, Wang N, Li Y, Cheng H, Chen Q (2014) Precipitation changes during the early Holocene and middle Holocene, implicated by exogenetic detrital mineral changes in Huahai Lake, Hexi Corridor of NW China. J Desert Res 34:1480–1485 **(in Chinese with English abstract)**

Li J, Hu X, Huang W, Wang J, Jiang J (2015a) Variation and trend prediction of the mountain runoffs of the trunk streams fo the Shule River Basin, Hexi Corridor. J Gliciol Geocryol 37:803–810 **(in Chinese with English abstract)**

Li Z, Wang N, Cheng H, Ning K, Zhao L, Li R (2015b) Formation and environmental significance of Late Quaternary calcareous root tubes in the deserts of the Alashan Plateau, Northwest China. Quat Int 372:167–174

Li Z, Wang N, Li R, Ning K, Cheng H, Zhao L (2015c) Indication of millennial-scale moisture changes by the temporal distribution of Holocene calcareous root tubes in the deserts of the Alashan Plateau, Northwest China. Palaeogeogr Palaeoclimatol Palaeoecol 440:496–505

Liu X, Herzschuh U, Shen J, Jiang Q, Xiao X (2008) Holocene environmental and climatic changes inferred from Wulungu Lake in northern Xinjiang, China. Quat Res 70:412–425

Liu B, Jin H, Sun L, Sun Z, Niu Q, Xie S, Li G (2014) Holocene moisture change revealed by the Rb/Sr ratio of aeolian deposits in the southeastern Mu Us Desert, China. Aeolian Res 13:109–119

Liu X, Lai Z, Madsen D, Zeng F (2015) Last deglacial and Holocene lake level variations of Qinghai Lake, northeastern Qinghai-Tibetan Plateau. J Quat Sci 30:245–257

Long H, Lai Z, Wang N, Li Y (2010) Holocene climate variations from Zhuyeze terminal lake records in East Asian monsoon margin in arid northern China. Quat Res 74:46–56

Long H, Lai Z, Fuchs M, Zhang J, Li Y (2012) Timing of Late Quaternary palaeolake evolution in Tengger Desert of northern China and its possible forcing mechanisms. Glob Planet Chang 92–93:119–129

Long H, Shen J, Tsukamoto S, Chen J, Yang L, Frechen M (2014) Dry early Holocene revealed by sand dune accumulation chronology in Bayanbulak Basin (Xinjiang, NW China). Holocene 24:614–626

Marcott SA, Shakun JD, Clark PU, Mix AC (2013) A reconstruction of regional and global temperature for the past 11,300 years. Science 339:1198–1201

Moore DM, Reynolds JC (1997) X-ray diffraction and the identification and analysis of clay minerals. Oxford University Press, New York

Morrill C, Overpeck JT, Cole JE (2003) A synthesis of abrupt changes in the Asian summer monsoon since the last deglaciation. Holocene 13:465–476

Nesbitt HW, Young GM (1989) Fommation and diagenesis of weathering profiles. J Geol 97:129–147

Opitz S, Wünnemann B, Aichner B, Dietze E, Hartmann K, Herzschuh U, Ijmker J, Lehmkuhl F, Li S, Mischke S, Plotzki A, Stauch G, Diekmann B (2012) Late Glacial and Holocene development of Lake Donggi Cona, north-eastern Tibetan Plateau, inferred from sedimentological analysis. Palaeogeogr Palaeoclimatol Palaeoecol 337–338: 159–176

Pedersen T, Calvert S (1990) Anoxia vs. productivity: what controls the formation of organic-carbon-rich sediments and sedimentary rocks? Aapg Bull 74:454–466

Ran M, Feng Z (2013) Holocene moisture variations across China and driving mechanisms: a synthesis of climatic records. Quat Int 313–314:179–193

Tapponnier P, Xu Z, Roger F, Meyer B, Arnaud N, Wittlinger G, Yang JS (2001) Geology-Oblique stepwise rise and growth of the Tibet plateau. Science 294:1671–1677

Wang N, Zhao Q, Li JJ, Hu G, Cheng H (2003) The sand wedges of the last ice age in the Hexi Corridor, China: paleoclimatic interpretation. Geomorphology 51:313–320

Wang Y, Cheng H, Edwards RL, He Y, Kong X, An Z, Wu J, Kelly MJ, Dykoski CA, Li X (2005) The Holocene Asian monsoon: links to solar changes and North Atlantic climate. Science 308:854–857

Wang K, Jiang H, Zhao H (2006) Advection and convergence of water vapor transport over the northwest China. Adv Water Sci 17:164–169 **(in Chinese with English abstract)**

Wang Y, Liu X, Herzschuh U (2010) Asynchronous evolution of the Indian and East Asian Summer Monsoon indicated by Holocene moisture patterns in monsoonal central Asia. Earth-Sci Rev 103:135–153

Wang N, Li Z, Cheng H, Li Y, Huang Y (2011) High lake levels on Alxa Plateau during the Late Quaternary. Chin Sci Bull 56:1799–1808

Wang N, Li Z, Li Y, Cheng H, Huang R (2012) Younger Dryas event recorded by the mirabilite deposition in Huahai lake, Hexi Corridor, NW China. Quat Int 250:93–99

Wang H, Chen Y, Li W, Deng H (2013a) Runoff responses to climate change in arid region of northwestern China during 1960–2010. Chin Geogr Sci 23:286–300

Wang N, Li Z, Li Y, Cheng H (2013b) Millennial-scale environmental changes in the Asian monsoon margin during the Holocene, implicated by the lake evolution of Huahai Lake in the Hexi Corridor of northwest China. Quat Int 313:100–109

Wang Y, Herzschuh U, Shumilovskikh LS, Mischke S, Birks HJB, Wischnewski J, Böhner J, Schlütz F, Lehmkuhl F, Diekmann B, Wünnemann B, Zhang C (2014) Quantitative reconstruction of precipitation changes on the NE Tibetan Plateau since the Last Glacial Maximum—extending the concept of pollen source area to pollen-based climate reconstructions from large lakes. Clim Past 10:21–39

Wang L, Li G, Dong Y, Han D, Zhang J (2015) Using hydrochemical and isotopic data to determine sources of recharge and groundwater evolution in an arid region: a case study in the upper-middle reaches of the Shule River basin, northwestern China. Environ Earth Sci 73:1901–1915

Wünnemann B, Mischke S, Chen F (2006) A Holocene sedimentary record from Bosten Lake, China. Palaeogeogr Palaeoclimatol Palaeoecol 234:223–238

Yao B, Liu X, Wang Y, Yang B (2011) Late Holocene climatic changes revealed by mineralogical records from lacustrine core KS-2006 from Lake Kusai in the Hoh Xil area, northern Tibetan Plateau. J Lake Sci 23:903–909 **(in Chinese with English abstract)**

Yuan D, Cheng H, Edwards RL, Dykoski CA, Kelly MJ, Zhang M, Qing J, Lin Y, Wang Y, Wu J, Dorale JA, An Z, Cai Y (2004) Timing, duration and transitions of the last interglacial Asian monsoon. Science 304:575–578

Zeng Y, Chen J, Xiao J, Qi L (2013) Non-residual Sr of the sediments in Daihai Lake as a good indicator of chemical weathering. Quat Res 79:284–291

Zhang H, Ma Y, Wünnemann B, Pachur HJ (2000) A Holocene climatic record from arid northwestern China. Palaeogeogr Palaeoclimatol Palaeoecol 162:389–401

Zhang H, Peng J, Ma Y, Chen G, Feng Z, Li B, Fan H, Chang F, Lei G, Wünnemann B (2004) Late Quaternary palaeolake levels in Tengger Desert, NW China. Palaeogeogr Palaeoclimatol Palaeoecol 211:45–58

Zhang J, Chen F, Holmes JA, Li H, Guo X, Wang J, Li S, Lü Y, Zhao Y, Qiang M (2011) Holocene monsoon climate documented by oxygen and carbon isotopes from lake sediments and peat bogs in China: a review and synthesis. Quat Sci Rev 30:1973–1987

Zhang X, Zhang C, Wu D, Zhou A (2015) Element geochenistry of lake deposits measured by X-ray fluorescence core scanner in northwest China. Mar Geol Quat Geol 35:163–174 **(in Chinese with English abstract)**